Master's thesis in biomathematics

The derivation of the functional response in a prey-predator system with active group defense

Anna Suomenrinne-Nordvik
Department of Mathematics and Statistics
University of Helsinki

2017

Supervisor: Stefan Geritz

HELSINGIN YLIOPISTO — HELSINGFORS UNIVERSITET — UNIVERSITY OF HELSINKI

Tiedekunta/Osasto — Fakultet/Sektion — Faculty	Laitos — Institution — Department
Matemaattis-luonnontieteellinen	Matematiikan ja tilastotieteen laitos

Tekijä — Författare — Author
Anna Suomenrinne-Nordvik

Työn nimi — Arbetets titel — Title

The derivation of the functional response in a prey-predator system with active group defense

Oppiaine — Läroämne — Subject		
Soveltava matematiikka		
Työn laji — Arbetets art — Level	Aika — Datum — Month and year	Sivumäärä — Sidoantal — Number of pages
Pro gradu -tutkielma	Joulukuu 2017	39 s.

Tiivistelmä — Referat — Abstract

Group defense against predator attacks are common for prey species. Some group defense mechanisms are more passive, like swarm confusion. In this thesis the focus is an active type of group defense where the prey fight back against the attacking predator as a group.

The aim of this thesis is to formulate a model with active groups defense and to mechanistically derive and analyse the functional response arising from it. The motivation is to understand the impact of this special type of group defense on the functional response of the predator, and hence on the whole dynamics of the model.

Some theory about prey-predator models, the functional response and tools for analysing dynamical systems are presented as background first. Following this, the model is formulated from the individual level processes and the functional response derived using the method of time-scale separation. Finally, two special cases of the model are analysed.

In the model, the defense of the prey is modelled as a coagulation and fragmentation process, where the prey can join the fight to protect the individual that is being attacked. These fights become clusters where the attacking predator is the coagulation kernel. The clusters can grow or shrink by one prey joining or leaving at a time, or the cluster breaking up completely due to success of either the attack or the defense. This type of coagulation and fragmentation process can be seen as a generalization of the Becker-Döring equations, where the clusters are homogenous groups and the groups can also only grow and shrink by one individual at a time.

The cluster dynamics truncated with a maximum size for the clusters was found to have a unique and stable equilibrium for arbitrarily large maximum cluster sizes in both special cases of the model. The stability analysis for cluster dynamics with no maximum cluster size was not successful, even though there is reason to believe the results for the truncated system is generalizable to that case.

The functional response was found to take a dome-shaped form, decreasing to zero under certain circumstances, or the form of Holling type II functional response. The determining factor for which type of functional response the model gives rise to is whether the predator's attack rate is dependent on the cluster size or not. The same dependence of the form of the functional response on the attack rate was found to hold in both special cases of the model.

Avainsanat — Nyckelord — Keywords
Prey-predator models, functional response, group defense, local stability analysis, time-scale separation, multi-scale analysis, coagulation and fragmentation processes, Perron-Frobenius theorem, Krein-Rutman theorem

Säilytyspaikka — Förvaringsställe — Where deposited
Kumpulan tiedekirjasto

Muita tietoja — Övriga uppgifter — Additional information

Contents

Chapter 1

Introduction

The aim of this thesis is to derive the functional response in a prey-predator system where the prey team up and actively defend against predator attacks. This dynamic was found to result in either a dome-shaped functional response, or a Holling type II functional response, depending on the predator capture rate.

A biological example of this type of interaction is the lion and the wildebeest. A wildebeest that is attacked by a lion may be joined by others from it's herd in an attempt to fight off the lion. The wildebeests are much bigger than the lion and have big horns, so the success of a lion against a large group is unlikely.

1.1 Prey-predator models

Prey-predator models are a useful and classical tool in studying ecological systems. They can be extended to a variety of resource-consumer or host-parasite interactions in nature, which makes studying the phenomenon occurring in such models interesting.

In mathematical modelling there is always a trade-off between detail and mathematical manageability. When formulating the model, the focus should be on the processes relevant to the questions asked and the point of view for the study, i.e. where the interest lies. Reality is of course always a lot more detailed than the model we choose to work with, but for mathematical purposes the details can be ignored or incorporated into the parameters. This is also done for methodological purposes, to link the individual-level processes to the population level phenomena, e.g. group formation to the shape of the functional response. Incorporating all possible processes into the model would make it a more realististic one, but it would make finding the link between the phenomena and processes more difficult. As a result of this, two models of the same ecological system with different objectives may look quite different from each other.

A well-known prey-predator model is the basic Lotka-Volterra model shown below [12] [17]. Here N denotes the prey density and P the predator density. The parameter α is the intrinsic growth rate of the prey population, i.e. the combined birth and death rate for the total population, β the rate at which the predator captures prey, γ the conversion constant of captured prey into new predator individuals and δ the death rate of the predator.

$$\begin{cases} \dot{N} = \alpha N - \beta NP \\ \dot{P} = \gamma NP - \delta P \end{cases} \tag{1.1}$$

The Lotka-Volterra model is an example of a very simple and not very realistic prey-predator model, because it assumes exponential growth for the prey when the predator is absent.

1.2 The functional response

The functional response is a key element in all ecological systems with predation. It contains the information about interaction between the resource and the consumer. The functional response is defined as the number of prey eaten by a single predator individual per unit of time. Typically this will be a function of the prey density, but it can also be dependent on the predator density. An example of this is the DeAngelis-Beddington functional response [4] [3].

This definition allows us to divide the modelled processes for both prey and predator into interaction between the species and population growth processes. A prey-predator model where the prey density is denoted by N and the predator density by P formulated using the functional response $f(N)$ can for example have the following form. This is the prey-predator model of Gause [5].

$$\begin{cases} \dot{N} = g(N)N - f(N)P \\ \dot{P} = \gamma f(N)P - \mu P \end{cases} \tag{1.2}$$

Here $g(N)$ is the predator-free prey population dynamics, including death and birth, γ is the conversion constant of eaten prey into offspring of the predator and μ the death rate of the predator. We see that the resulting dynamics for both predator and prey will depend on the functional response of the predator as much as on the processes indepedent of the inter-species interactions. This is characteristic for the functional response and makes it's impact on the dynamics an interesting element to study.

1.3 Types of functional responses

There are several well-known types of functional responses, each of them resulting from different underlying individual-level processes. The most well-known functional response types are Holling type I and type II [9]. In this section I will present four classifications of functional responses.

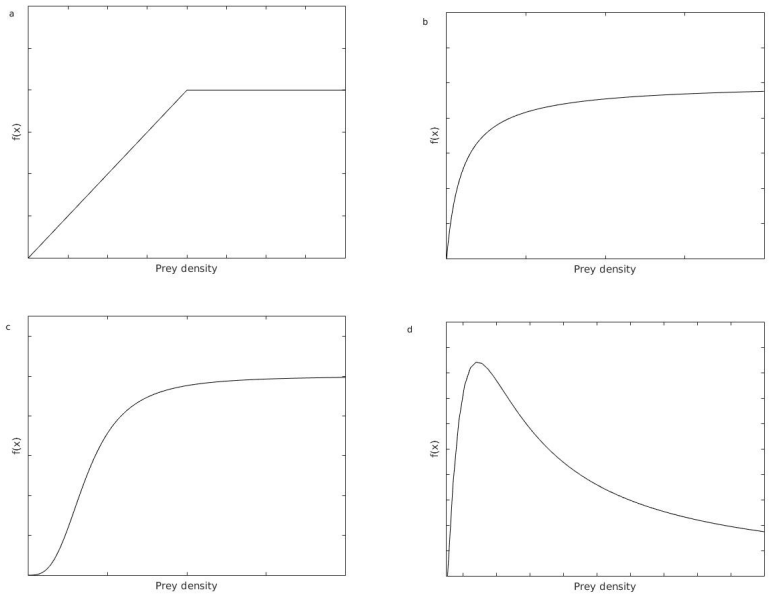

Figure 1.1: Graphical representation of the four most well-known functional responses. a: Holling Type I or linear (here shown with saturation), b: Holling Type II, c: Holling Type III and d: The functional response derived and studied in this thesis, also called non-monotonous or dome-shaped functional response.

1.3.1 Monotonous functional responses

The three classifications of functional responses made by Holling are all monotonous functions of the prey density. There are several different models with different interaction processes that give rise to these three types of functional responses.

The functional response known as the Holling type I, seen in figure 1.1 a, is a linear and saturating function of the prey density. The simple Lotka-Volterra model shown in (1.1) on page 3 gives a Holling type I functional response. The functional response of the Lotka-Volterra equations takes the form of $f(N) = \beta N$, but it can be assumed to saturate for very high prey densities for increased realism.

The Holling type II functional response, figure 1.1 b, is also a saturating function of prey density, but it has the added assumption of the predator population being divided into searching and handling individuals. In models with this assumption, only the searching predator individuals attack prey and the handling individuals spend their time digesting and resting etc. Searching predators enter the handling class after capture of a prey and handling predators go back to the searching class after some time. This leads to the type II functional response given by $f(N) = \frac{\alpha N}{1+\alpha h N}$, α being the attack rate of the searching predator and h the expected handling time of a handling predator before returning to the searching class.

Other processes, in particular those studied in this thesis, also lead to the Holling type II functional response. That means the functional response is qualitatively the same but with a different mathematical expression.

Type III of the Holling functional responses, figure 1.1 c, takes an s-form before saturating. In some models this is a result of the predator learning how to capture prey when prey densities are low and predation increasing more rapidly as the learned behaviour spreads in the predator population as the prey population increases. The function that gives type III is of the form

$$f(N) = \frac{\alpha N^n}{1 + \alpha h N^n} \ , \tag{1.3}$$

where $n > 1$ and the parameters α and h might consist of multiple model parameters. Leslie Real pointed out in a paper from 1977 that Type I and II functional responses are special cases of the equation (1.3), where $h = 0$ and $n = 1$ for type I and $h \neq 0$ and $n = 1$ for type II [16].

1.3.2 Non-monotonous functional responses

There have also been observed non-monotonous functional responses, which reach their maximum value at a certain prey density and decrease after that. These types of functional responses are sometimes called the type IV (not classified by Holling) but are also referred to as the humpback, dome-shaped or unimodal functional response. An example can be seen in figure 1.1 d. Non-monotonous functional responses can occur in models with swarm confusion [10] and other group defense mechanisms.

The classification of functional responses is not very accurate since many different models with different processes give rise to them and the divide between them is sometimes unclear. The advantage of classifying the functional responses is that many types of functional responses have been well studied, and once you know what type of functional response a model has you have an indication of the resulting dynamics.

1.4 Stability analysis of dynamical systems

When analysing dynamical systems, one often wants to find the equilibrium solution, i.e. the solution that does not change in time. One important aspect of equilibria is whether a small perturbation to it causes the trajectory of the system to move back to the equilibrium or if it moves away from it. If any small preturbation of the equilibrium goes back to the equilibrium, it is said to be stable. Moreover, an equilibrium that is attracting and stable is called a globally asymptotically stable equilibrium.

There are a vast variety of tools, results and theories related to stability of equilibrias in dynamical systems, however in this thesis I only use linear stability analysis.

Linear stability analysis

The stability theory developed by Lyapunov [13] states that for a linear dynamical system a hyperbolic equilibrium is globally, asymptotically stable if all the eigenvalues of it's Jacobi matrix have strictly negative real parts at the equilibrium value.

The Jacobi matrix of a system is the matrix of all partial derivatives of the system $J(x) = \left[\frac{\partial f_{ij}}{\partial x_{ij}}(x)\right]$. An equilibrium is hyperbolic if the Jacobi matrix has no eigenvalues with zero real part.

The Hartman-Grobman theorem generalises this result to non-linear systems. The theorem states that a non-linear system is locally topologically equivalent to it's linearisation around a hyperbolic equilibrium point [8] [7].

1.5 Time-scale separation

One of the first and most well-known examples of the use of time-scale separation within a dynamical system was in 1913 by Michealis and Menten in a biochemistry setting [15]. It is a method for reducing the dimension of the system to make it easier to analyse. In this section I will describe the method in a three-dimensional system so it can be used in later sections without detailed explanation of each step.

Time-scale separation is based on prior knowledge of the relative rates of change of the different densities in the system. One property of a system which warrants the use of the method is if one density in the system is much larger than the others. In a short span of time the relative change in a large density will be much smaller than in a small. E.g. a change of one unit is a change of 0.1% for a density of 1000 units, but for a density of single unit it's a change of 100%. Another property allowing for the method to be used is if one or more of the processes are much faster than others. Compare a process happening at a rate of 100 per unit of time to a process happening at a rate of 0.1 per unit of time.

What is done to highlight this difference is scaling the time which is examined.

Example

Consider a prey-predator system where the predators are divided into searching S and handling H predators and the prey density is denoted by N. Only the hunting interactions are considered, i.e. reproduction and predation-independent deaths are omitted. Searching predators attack a prey with rate α and go into the handling state. From the handling state they become a searching predator again with rate $\frac{1}{h}$.

$$\begin{cases} \frac{\mathrm{d}N}{\mathrm{d}t} & = -\alpha SN \\ \frac{\mathrm{d}S}{\mathrm{d}t} & = -\alpha SN + \frac{1}{h}H \\ \frac{\mathrm{d}H}{\mathrm{d}t} & = \alpha SN - \frac{1}{h}H \end{cases}$$

The total predator density denoted by P is constant in this model and is the sum of the searching and handling predator densities. We rewrite the system in terms of the total predator density.

$$\begin{cases} \frac{\mathrm{d}N}{\mathrm{d}t} & = -\alpha SN \\ \frac{\mathrm{d}P}{\mathrm{d}t} & = 0 \\ \frac{\mathrm{d}S}{\mathrm{d}t} & = -\alpha SN + \frac{1}{h}(P - S) \end{cases} \tag{1.4}$$

We now assume that the predator density is much smaller than the density of prey. This is a reasonable assumption to make. We introduce the small dimensionless scaling parameter $\epsilon > 0$. We do this to scale the predator density up to a scale where it is comparable to the bigger prey density.

$$S^* = \frac{S}{\epsilon} \qquad P^* = \frac{P}{\epsilon} \quad \Leftrightarrow \quad S = \epsilon S^* \quad P = \epsilon P^*$$

Rewriting the equations, the dynamical system becomes the following.

$$\begin{cases} \frac{\mathrm{d}N}{\mathrm{d}t} & = -\alpha\epsilon S^* N \\ \epsilon\frac{\mathrm{d}P^*}{\mathrm{d}t} & = 0 \\ \epsilon\frac{\mathrm{d}S^*}{\mathrm{d}t} & = -\alpha\epsilon S^* N + \frac{1}{h}(\epsilon P^* - \epsilon S^*) \end{cases} \tag{1.5}$$

Letting ϵ go to zero, we get the following system. Note that ϵ cancels out in the equations for P^* and S^*. According to singular perturbation theory, the dynamical systems (1.4) and (1.5) are topologically equivalent for small ϵ.

$$\begin{cases} \frac{\mathrm{d}N}{\mathrm{d}t} & = 0 \\ \frac{\mathrm{d}P^*}{\mathrm{d}t} & = 0 \\ \frac{\mathrm{d}S^*}{\mathrm{d}t} & = -\alpha S^* N + \frac{1}{h}(P^* - S^*) \end{cases} \tag{1.6}$$

From this fast dynamic we get the quasi-equilibrium value for the density of searching predators.

$$\hat{S^*} = \frac{P^*}{1 + \alpha h N}$$

The idea of time-scale separation is that the fast dynamics equilibriate before the change on the slower time-scale starts to play a role. To use the quasi-equilibrium, we must make sure that it is hyperbolically stable on the fast time-scale, otherwise there is no reason why the system should converge to it in fast time. We find that the Jacobian of the fast system (1.6) has one distinct, real and negative eigenvalue.

$$\lambda = -(\alpha N + \frac{1}{h})$$

This means that the quasi-equilibrium is stable on the fast time-scale. To see what happens on the slower time-scale, we now scale the time of system (1.5).

$$t^* = \epsilon t \Leftrightarrow \frac{\mathrm{d}}{\mathrm{d}t^*} = \frac{\mathrm{d}}{\mathrm{d}t}\frac{\mathrm{d}t}{\mathrm{d}t^*} = \frac{\mathrm{d}}{\mathrm{d}t}\frac{1}{\epsilon}$$

$$\begin{cases} \frac{\mathrm{d}N}{\mathrm{d}t^*} & = \frac{1}{\epsilon}(-\alpha\epsilon S^* N) \\ \frac{\mathrm{d}P^*}{\mathrm{d}t^*} & = 0 \\ \epsilon\frac{\mathrm{d}S^*}{\mathrm{d}t^*} & = \frac{1}{\epsilon}(-\alpha\epsilon S^* N + \frac{1}{h}\epsilon(\epsilon P^* - \epsilon S^*)) \end{cases}$$

Letting ϵ go to zero again, the dynamics on the slow time-scale becomes the following. We see that on the slow time-scale, S doesn't change and the equation is the quasi-equilibrium equation, so we can substitute the quasi-equilibrium of S into the equation for the prey.

$$\begin{cases} \frac{dN}{dt^*} & = -\alpha S^* N \\ \frac{\mathrm{d}P^*}{\mathrm{d}t^*} & = 0 \\ 0 & = -\alpha S^* N + \frac{1}{h}(P^* - S^*) \end{cases}$$

$$\Leftrightarrow$$

$$\frac{dN}{dt^*} = -\alpha\hat{S^*}N = -\frac{\alpha P^*}{1 + \alpha h N}N = -f(N)P^*$$

Now we have derived the functional response of the predator, $f(N) = \frac{\alpha N}{1+\alpha h N}$, using the method of time-scale separation. This is the Holling type II response.

1.6 Coagulation and fragmentation processes

A special type of interactions in many types of models are coagulation and fragmentation processes. They describe the the growth and decline in size of groups of particles of some kind e.g. water droplets.

An example of these processes are the Becker-Döring equations [2]. The Becker-Döring equations, seen below, describe homogeneous groups that can either grow by one or shrink by one unit at a time.

$$
\begin{cases}
\dot{n_1} & = -a_1 x_1 n_1 + b_2 n_2 - \sum_{k=1}^{K-1} (a_k n_k n_1 + b_{k+1} n_{k+1}) \\
\dot{n_2} & = a_1 n_1 n_1 + b_3 n_3 - a_2 n_2 n_1 - b_2 n_2 \\
\vdots & \\
\dot{n_k} & = a_{k-1} n_{k-1} n_1 + b_{k+1} n_{k+1} - a_k n_k n_1 - b_k n_k \qquad \text{for } 1 < k < K \\
\vdots & \\
\dot{n_K} & = a_{K-1} n_{K-1} n_1 - b_K n_K
\end{cases} \tag{1.7}
$$

A group of k units grows with rate $a_k x_1$, where x_1 is the density of single units, and shrinks with rate b_k. The rates can depend on the size of a group, and the groups may have a maximum size K, from which they can no longer grow.

Note that the groups of size one play a special role, since the groups only grow and shrink by one unit at a time. That means that growth and decline in any group size reduces or increases the density of single particles.

The Becker-Döring equations are known to have a unique and stable equilibrium.

1.7 The model of Geritz and Gyllenberg

An example of a prey-predator model that has a coagulation and fragmentation process is a model by Geritz and Gyllenberg [6]. In the model the prey defend themselves from a predator that can only attack single prey individuals by forming groups. Here, the group formation process follows the Becker-Döring equations.

The group formation processes are assumed to be on a faster time-scale than prey capture and also the population level processes. The group formation equations are the same as in equations (1.7) and since there is no birth or death, the total prey density is constant $N = \sum_{k=1}^{K} k n_k$.

The quasi-equilibrium of the group formation dynamics is then the following.

$$\hat{n_k} = Q_k \hat{n_1}^k \ , \qquad \text{where} \tag{1.8}$$

$$Q_k = \prod_{i=1}^{k-1} \frac{a_i}{b_{i+1}} \qquad (Q_1 = 1)$$

The Lyapunov function

$$V = \sum_{k=1}^{K} n_k \left(\log\left(\frac{n_k}{Q_k} \right) - 1 \right)$$

proves the global asymptotic stability of the equilibrium.

Since the total prey density is constant on the group fromation time-scale, it may be expressed in terms of the quasi-equilibrium (1.8). It then becomes an expression dependent on the density of single prey individuals, or more precisely, the density of single prey depends on the total prey density.

$$N = \sum_{k=1}^{K} k Q_k \hat{n_1}^k \quad \Leftrightarrow \quad \hat{n_1}(N)$$

The equilibrium group size distribution is illustrated in the figure 1.2.

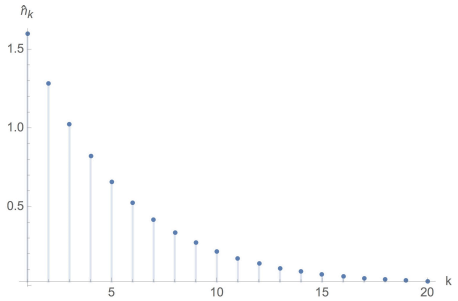

Figure 1.2: The equilibrium distribution plotted with constant rates $\frac{a}{b} = 0.5$ and maximum group size $K = 20$.

If the predator has a constant capture rate of single prey β, the functional response becomes of Holling type II in the limit $K \to \infty$.

$$f(N) = \beta \hat{n_1}(N)$$

If the full prey-predator dynamics is taken to be the following quite simple model, the dynamics of the system becomes the same as in the well-studied model of Rosenzweig and MacArthur [14]. Here the predator free dynamics of the prey is the logistic growth function $g(N) = rN(1 - N/K)$, and the predator has a conversion constant of captured prey into offspring γ and a death rate δ. The prey-predator dynamics of this model show a Hopf bifurcation and a limit cycle, which would not exist for a model without prey group formation.

$$\begin{cases} \dot{N} = g(N)N - f(N)P \\ \dot{P} = \gamma f(N)P - \delta P \end{cases}$$

The model and analysis of Geritz and Gyllenberg show that the coagulation and fragmentation process has a significant impact on the full dynamics of the model, and that it is a good approach to modelling group defense of prey.

The model formulated in this thesis is similar to the model of Geritz and Gyllenberg with the prey defense mechanism being a coagulation and fragmentation process. However in the model of this thesis the prey defense is a more active one, with direct interference with the attack of the prey instead of an attempt at avoiding being attacked in the first place.

Chapter 2

Model formation

Now we want to formulate a model as described in the introduction. In order to do that we have to specify the individual level, i-level, processes first. This model consists of prey, searching predator, and handling predator individuals. During an attack predators and prey form clusters of one predator and k prey defending against the attack ($k \in 1, 2, \cdots, K$). The density of clusters of size k is denoted by P_k and maximum cluster size K can be taken to be infinite in some cases. Prey density is denoted by N, searching predator density by S and handling predator density by H. When a prey is killed, the predator goes from being in a cluster to handling state, where it digests and rests for an exponentially distributed handling time. The kill may result in an offspring for the predator.

In the first section of this chapter I will elaborate on how the cluster dynamics is modelled and in the second section the full dynamics of the model will be explained.

2.1 Modelling prey cooperation as active defense

The cooperation of prey against predator attacks is modelled as a coagulation and fragmentation processes. When a predator attacks a prey, they form a pair. Other prey can then join this pair in an effort to fend off the predator, forming a cluster of one predator and several prey individuals. Prey individuals may leave the cluster before the fighting is over, shrinking the cluster size by one at a time, or the predator may give up causing the cluster to fully break up. In the case of prey capture (only one prey from the cluster is assumed to be captured) the cluster also breaks apart.

Note that in this process the single predator is the kernel around which the cluster forms, growing and shrinking only by one prey individual at a time or by bursting due to prey failure or success in the defense. These cluster growth and shrinking processes are a

sort of generalized version of the Becker-Döring processes.

In these clusters only searching, i.e. hunting predators are present. A single searching predator is denoted by P_0, as in a cluster with zero prey, and the total density of searching predators is $S = \sum_{k=0}^{K} P_k$, since all clusters of all sizes contain exactly one predator.

A single searching predator, P_0, attacks a free prey, N, at rate a_0 and the pair become a cluster of size one, P_1. A free prey joins a cluster of size k with rate a_k and leaves it with rate b_k, increasing and shrinking the cluster size with one respectively. A cluster of size k breaks up with rate c_k due to the predator giving up, upon which the predator goes back to searching as a single predator and the k prey go back to being free prey. With rate β_k the predator makes a kill in a cluster of size k, upon which the predator becomes a handling predator, H, and $(k-1)$ prey go back to being free prey. All the parameters are positive, but may become zero for some value of k. For example the capture rate β_k must be decreasing as k increases, at least after a threshold value of k, to keep the model as a good interpretation of reality.

Below the figure (2.1) describes the i-level processes in clusters and the corresponding set of differential equations for cluster dynamics are given below that.

(2.1)

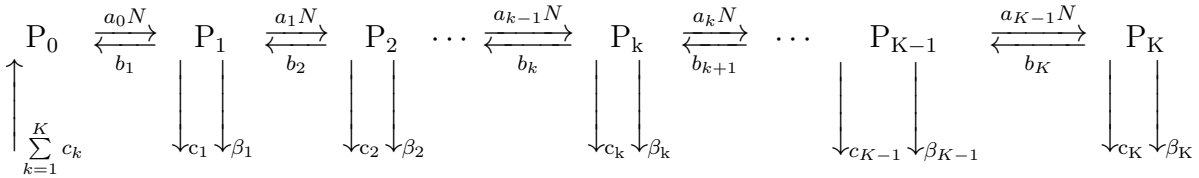

$$
\begin{cases}
\dot{P}_0 = -a_0 N P_0 + b_1 P_1 + \sum_{k=1}^{K} c_k P_k \\
\dot{P}_k = a_{k-1} N P_{k-1} - a_k N P_k + b_{k+1} P_{k+1} - b_k P_k - c_k P_k - \beta_k P_k \qquad \text{for } 0 < k < K \\
\dot{P}_K = a_{K-1} N P_{K-1} - b_K P_K - c_K P_K - \beta_K P_K \\
\dot{N} = -\sum_{k=0}^{K-1} a_k N P_k + \sum_{k=1}^{K} k\, c_k P_k + \sum_{k=1}^{K} (k-1) \beta_k P_k \\
\dot{H} = \sum_{k=1}^{K} \beta_k P_k
\end{cases}
$$

This type of cluster dynamic can be seen as a generalized version of the Becker-Döring process, where the possibility of clusters bursting is added as opposed to the restriction to changes by one unit only. Also the Becker-Döring equations describe changes in groups in homogeneous populations, whereas here there is a coagulation kernel of a different type to the individuals clustering around it.

2.2 The full model

The remaining i-level processes yet to be added to the model are birth and death. For the prey, the predator-free dynamics are left unspecified and denoted as function $g(N)$, which can be any realistic population dynamic. The handling predators have handling time h, corresponding to a rate $\frac{1}{h}$ of returning to the searching single predator state. Predators have natural death rate δ in both searching and handling state. In this model it's considered unlikely that the predator dies mid-hunt of natural causes so it's dropped from the cluster equations. The prey could kill the predator while defending against the attack, and that could be added as an individual process breaking up the clusters, but for now the risk of hunting is just considered to raise the average death rate δ. Predator birth is modelled through a conversion constant of ρ per killed prey, where the new individuals enter straight into the population of searching single predators. The parameter ρ ($0 < \rho \leq 1$) can be interpreted as the probability of a birth given a kill.

Adding these processes into the model gives the differential equations (2.2) below for the full model.

(2.2)
$$
\begin{cases}
\dot{N} = g(N)N - \sum_{k=0}^{K-1} a_k N P_k + \sum_{k=1}^{K} k\, c_k P_k + \sum_{k=1}^{K} (k-1)\beta_k P_k \\
\dot{H} = \sum_{k=1}^{K} \beta_k P_k - \frac{1}{h} H - \delta H \\
\dot{P_0} = -a_0 N P_0 + b_1 P_1 + \sum_{k=1}^{K} c_k P_k + \rho \sum_{k=1}^{K} \beta_k P_k + \frac{1}{h} H - \delta P_0 \\
\dot{P_k} = a_{k-1} N P_{k-1} - a_k N P_k + b_{k+1} P_{k+1} - b_k P_k - c_k P_k - \beta_k P_k \qquad \text{for } 0 < k < K \\
\dot{P_K} = a_{K-1} N P_{K-1} - b_K P_K - c_K P_K - \beta_K P_K
\end{cases}
$$

Now that we have defined our model, we will in the next chapter derive the resulting functional response of the predator. As a consequence of knowing the expression for the functional response, the dynamical system for the full model will be significantly simplified as seen in (1.2), which will make analysing the full population dynamics a lot easier.

Conclusion
In the model, the defense of the prey is modelled as a coagulation and fragmentation process, where the prey can join the fight to protect the individual that is being attacked. These fights become clusters where the attacking predator is the coagulation kernel. The clusters can grow or shrink by one prey joining or leaving at a time, or the cluster breaking up completely due to success of either the attack or the defense. This type of coagulation and fragmentation process can be seen as a generalization of the Becker-Döring equations, where the clusters are homogenous groups and the groups can also only grow and shrink by one individual at a time.

Chapter 3

Deriving the functional response

3.1 The functional response

The functional response is the number of prey captured per unit of time per predator individual. To get an explicit expression for the functional response, we need the total number of prey captured per unit of time and the total number of predators. The full model (2.2) is a huge system. In order to make sense of it we should take steps to simplify it. To this end, we make a time-scale separation based on some realistic assumptions.

The first assumption is that the prey density is much larger than the predator density. This is a common assumption to make in ecology for prey-predator models. It has the consequence that the prey population changes slowly relative to predator density. The second assumption is that birth and death processes are slow compared to the rest of the processes, meaning that individuals die and are born less often than they for example eat. In other words, the rates a_k, b_k, c_k, β_k and $\frac{1}{h}$ are of a larger order of magnitude than ρ and δ.

$$\begin{aligned} &(1) \qquad N >> S + H \\ &(2) \qquad a_k, b_k, c_k, \beta_k, \frac{1}{h} >> \rho, \delta \end{aligned}$$

This results in a time-scale separation between the full population dynamics and the searching-handling cycle dynamics, the latter being the faster system, which is given by the set of differential equations (3.1).

(3.1)
$$\begin{cases} \dot{N} = 0 \\ \dot{H} = \sum_{k=1}^{K} \beta_k P_k - \frac{1}{h} H \\ \dot{P}_0 = -a_0 N P_0 + b_1 P_1 + \sum_{k=1}^{K} c_k P_k + \frac{1}{h} H \\ \dot{P}_k = a_{k-1} N P_{k-1} - a_k N P_k + b_{k+1} P_{k+1} - b_k P_k - c_k P_k - \beta_k P_k \qquad \text{for } 0 < k < K \\ \dot{P}_K = a_{K-1} N P_{K-1} - b_K P_K - c_K P_K - \beta_K P_K \end{cases}$$

We note now that the total predator density is $P_T = H + S$, where $S = \sum_{k=0}^{K} P_k$, and the total number of captured prey per unit of time is exactly the number of clusters breaking up due to capture per unit of time, i.e. $\sum_{k=1}^{K} \beta_k P_k$. Since these are all on a faster time-scale than the birth and death processes, we can solve the quasi-equilibrium for them and, given that they are stable quasi-equilibriums, use them to express the functional response.

$$f(N, P_T) = \frac{\sum_{k=1}^{K} \beta_k \hat{P}_k}{\sum_{k=0}^{K} \hat{P}_k + \hat{H}}$$

However, solving the equilibriums of system (3.1) is still not a straightforward task. I will argue that it's possible to make a further time-scale separation without making unreasonable assumptions. Firstly, the handling time of predators hunting big prey tend to be at least a few days, and the attacks of the predator happen in bursts of energy, lasting only a few minutes. Secondly, prey capture is a relatively rare event and most prey-predator interactions end in the hunted getting away.

This results in a second time-scale separation between the searching-handling cycle and an even faster dynamic given by the following dynamical system. This fast dynamics (3.2) is the cluster dynamics described in figure (2.1), only without prey capture.

$$
(3.2)\qquad \begin{cases} \dot{N} = 0 \\ \dot{H} = 0 \\ \dot{P}_0 = -a_0 N P_0 + b_1 P_1 + \sum_{k=1}^{K} c_k P_k \\ \dot{P}_k = a_{k-1} N P_{k-1} - a_k N P_k + b_{k+1} P_{k+1} - b_k P_k - c_k P_k \qquad \text{for } 0 < k < K \\ \dot{P}_K = a_{K-1} N P_{K-1} - b_K P_K - c_K P_K \end{cases}
$$

On this time-scale the densities of both prey N and handling predators H are constant. Also the density of searching predators, i.e. the total number of clusters, $S = \sum_{k=0}^{K} P_k$, is constant because there is no death or birth of predators on the time-scale of cluster dynamics.

Given that we can solve the equilibrium distribution of P_k clusters in the cluster dynamics system (3.2), denoted by $\hat{P}_k$, where $0 \leq k \leq K$, we will have almost everything we need for writing out the functional response explicitly. The quasi-equilibrium of the handling predator density on the searching-handling cycle time-scale (3.1) is easily solved using the equilibrium distribution $\hat{P}_k$.

$$
\hat{H} = h \sum_{k=1}^{K} \beta_k \hat{P}_k
$$

To express the functional response using the quasi-equilibriums we need to prove that they are stable. Given that $\hat{P}_k$ is stable, it follows that the quasi-equilibrium of H on the searching-handling cycle time-scale is stable. The stability is quickly confirmed by observing that the differential equation for H is a single first order linear differential equation with a single negative eigenvalue of the Jacobi matrix when the system on the cluster dynamic time-scale has equilibrated.

We now have the information we need to formulate the expression of the functional response for this model. The dependence of the functional response on the densities of prey and predators depends on the form of the quasi-equilibrium $\hat{P}_k$.

$$f(N,S) = \frac{\sum_{k=1}^{K} \beta_k \hat{P}_k}{\sum_{k=0}^{K} \hat{P}_k + h \sum_{k=1}^{K} \beta_k \hat{P}_k} \qquad \text{where } S = \sum_{k=0}^{K} P_k \tag{3.3}$$

In the next sections I will derive the explicit form of the quasi-equilibrium distributions, show their stability and look at the resulting functional responses for two special cases for the rates a_k, b_k and c_k of the cluster dynamics. The full model is too general to say anything meaningful about without prior knowledge of what the parameters for the different cluster sizes are. The set of all possible parameter combinations is so big that a huge variety of dynamics can be engineered by choosing the right parameters.

3.2 Special case: constant cluster dynamic rates

In this section I solve the quasi-equilibriums and explicit form of the functional response in the case of constant rates a, b and c on the cluster dynamic time-scale. For this case, all three parameters are non-zero. Note that if $c = 0$ we are back to the Becker-Döring processes, which are well studied and not included here. The case of $b = 0$, I leave for the next section on another special case of the generic cluster dynamic model 3.2. If the parameter a is equal to zero, the model becomes uninteresting, since the predator never attacks and thus starves to death.

The equilibrium equations of the cluster dynamics can be expressed in the following form for constant cluster parameters. Since the searching predator density is constant on this time-scale, the equation for $\hat{P}_0$ can be omitted and solved using the expression for the $\hat{P}_k$ densities.

$$0 = aNP_k - (aN + b + c)P_{k+1} + bP_{k+2} \qquad \text{for } k \geq 0 \tag{3.4}$$

This three-parameter linear recurrence equation can be reduced to a two-parameter equation by substituting $\alpha = \frac{aN}{b}$ and $\gamma = \frac{c}{b}$. Note that since $b = 0$ is ruled out for now, we can do this.

$$0 = \alpha P_k - (\alpha + 1 + \gamma)P_{k+1} + P_{k+2} \tag{3.5}$$

For this linear equation, there exists a general solution (3.6) depending on the eigenvalues. The eigenvalues are solved from the characteristic equation (3.7). Although we have a general solution, we need to make sure the solutions stay positive and real as they

are expressions for population densities. If the maximum cluster size K can be infinity, the solution must converge, which means that the eigenvalue used must be less than unity.

$$\hat{P}_k = \begin{cases} A\,\lambda_+^k + B\,\lambda_-^k & \text{if } \lambda_+ \neq \lambda_- \\ (A + Bk)\lambda^k & \text{if } \lambda_+ = \lambda_- = \lambda \end{cases} \quad \text{for arbitrary constants } A, B \in \mathbb{C}\,. \tag{3.6}$$

$$0 = \alpha\,\lambda^k - (\alpha + 1 + \gamma)\lambda\,\lambda^k + \lambda^2\,\lambda^k \quad \Leftrightarrow \quad 0 = \alpha - (\alpha + 1 + \gamma)\lambda + \lambda^2 \tag{3.7}$$

$$\lambda_\pm = \frac{1}{2}\left(1 + \alpha + \gamma \pm \sqrt{(1 + \alpha + \gamma)^2 - 4\alpha}\right)$$

The eigenvalues are always real and never equal. If we assume they are not we get a contradiction.

$$\begin{aligned} (1 + \alpha + \gamma)^2 &\leq 4\alpha \\ (1 + \frac{aN}{b} + \frac{c}{b})^2 &\leq 4\frac{aN}{b} \\ (1 - \frac{aN}{b})^2 + \frac{c}{b}\left(2 + 2\frac{aN}{b} + \frac{c}{b}\right) &\leq 0 \end{aligned}$$

The last equation above shows that the eigenvalues are equal only when $\alpha = 1$ and $\gamma = 0$. But we already assumed that none of the parameters are zero, so that's a contradiction. Also, the left hand side of the last equation is clearly positive, so the eigenvalues must be real for all positive values of the parameters.

In addition λ_+ is greater than or equal to one and λ_- is less than or equal to one for all possible parameter values. Equality to one for both eigenvalues only happens when γ is zero. In figure 3.1 the two eigenvalues are shown plotted with the unit surface.

Assuming that there is no upper bound on cluster size, we must use λ_- for convergence of the solution. The expression of the solution then becomes the following.

$$\hat{P}_k = C\lambda_-^k$$

From the equilibrium equation for P_0, we get the value for C. The equilibrium is unique because of the linearity of the equations. The stability analysis of this equilibrium on the time-scale of the cluster dynamics can be found in section 3.2.2. From here on, I will make the dependence of the eigenvalue λ_- on the prey density N explicit by denoting it by $\lambda_-(N)$. This I do to make the connection between the equilibrium cluster densities and the prey density clear.

$$\hat{P}_k = \lambda_-(N)^k \hat{P}_0 \quad \text{for } k \geq 0$$

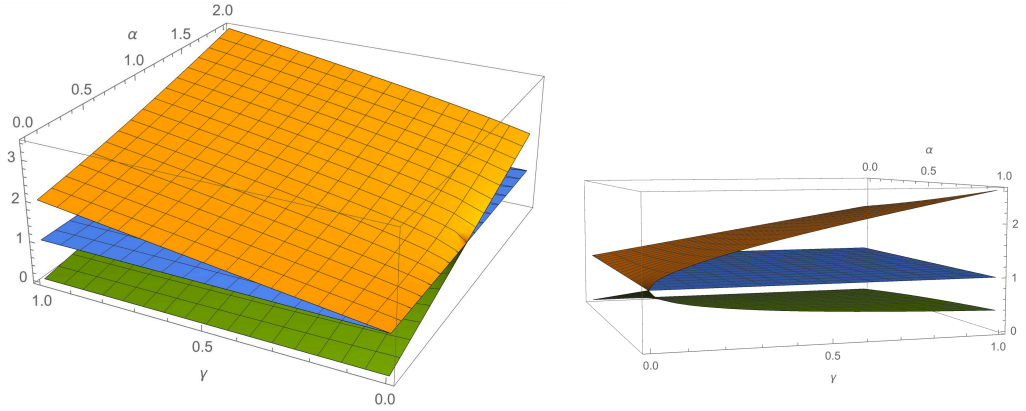

Figure 3.1: The upper surface is the eigenvalue λ_+ and the lower surface is the eigenvalue λ_-. The middel surface equals 1. Note that the eigenvalues are not equal to each other or to 1 anywhere for $\gamma > 0$.

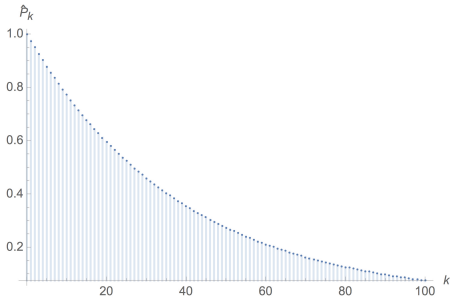

Figure 3.2: The equilibrium distribution plotted with parameter values $\frac{\alpha}{N} = 0.2$, $N = 100$, $\gamma = 0.5$, $P_0 = 1$ and maximum cluster size $K = 100$.

The quasi-equilibrium distribution of the different sized clusters is shown in figure 3.2.

Now we substitute the expression for the quasi-equilibrium into the expression for the functional response (3.3) on page 19. The functional response only depends on the density of free prey and is equal to (3.8) below.

$$f(N) = \frac{\sum_{k=1}^{\infty} \beta_k \, \lambda_-(N)^k \hat{P}_0}{\sum_{k=0}^{\infty} \lambda_-(N)^k \hat{P}_0 + h \sum_{k=1}^{\infty} \beta_k \, \lambda_-(N)^k \hat{P}_0} = \frac{\sum_{k=1}^{\infty} \beta_k \, \lambda_-(N)^k}{\sum_{k=0}^{\infty} \lambda_-(N)^k + h \sum_{k=1}^{\infty} \beta_k \, \lambda_-(N)^k} \tag{3.8}$$

Remark

In the limit for $N \to \infty$, $\lambda_-(\mathrm{N})$ becomes one, for all positive values of α and γ. The expression also approaches the limit from below, since we know it's always between zero and one. This is illustrated in figure 3.3.

These properties allow us to make the first substitution below for the converging geometric series $\sum_{k=0}^{\infty} \lambda_-(N)^k$.

$$S = \sum_{k=0}^{\infty} \lambda_-(N)^k \hat{P}_0 = \frac{1}{1-\lambda_-(N)} \hat{P}_0 \quad \Leftrightarrow \quad \frac{S}{\hat{P}_0} = \frac{1}{1-\lambda_-(N)}$$

Rearranging the terms like on the right hand side above, we see that in the limit for $N \to \infty$, $\frac{S}{\hat{P}_0}$ becomes infinite. As our S, the total searching predator density on the time-scale of the cluster dynamics, is a constant, the equality can only hold if $\hat{P}_0$ becomes zero in the limit $N \to \infty$.

As the quasi-equilibrium expression for all cluster size densities is multiplied by $\hat{P}_0$, we see that in the limit for $N \to \infty$ all cluster size densities $\hat{P}_k$ become zero.

Consequently, in the limit $N \to \infty$ the quasi-equilibrium distribution of cluster sizes becomes the uniform distribution over all natural numbers with density zero. However, this does not mean that the clusters disappear, but they are growing to the next size at an "infinite rate" ($aN \to \infty$), i.e. all the mass of the distribution escapes to $+\infty$.

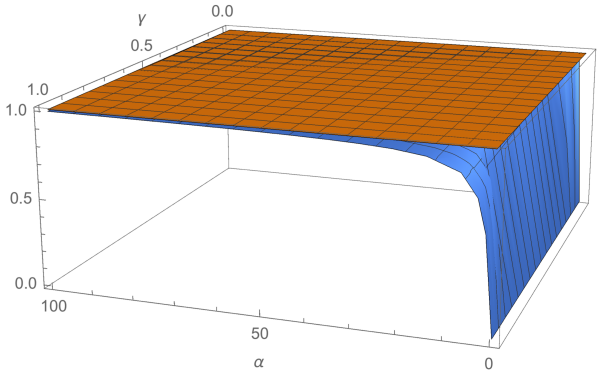

Figure 3.3: The limit of the eigenvalue $\lambda_-(N)$ as N grows, illustrated. The upper surface equals to 1 and the lower surface to $\lambda_-(N)$. ($N \to \infty \Leftrightarrow \alpha = \frac{aN}{b} \to \infty$)

Of course, this does not happen in real life, but from this reasoning we get an idea of how the cluster size distribution is affected by prey population growth. Compare the example of a distribution in figure 3.2 on the previous page where $N = 100$, with the uniform zero distribution in the limit $N \to \infty$.

3.2.1 The shape of the functional response

In the case of constant cluster rates, the shape of the functional response depends strongly on the capture rate of the predator β_k. Here I consider three types of capture rates to be realistic, which are shown in figure 3.4.

The functions for the rates are chosen such that they take a form that is considered realistic, a derivation of them from i-level processes is out of the scope of this thesis, although preferable to this approach. The functions used for the different types of capturing rates are listed below.

(a)	$\beta_k = \psi$	Constant capture rate.
(b)	$\beta_k = \frac{\omega k+1}{\phi k^2+\psi k} + 0.5$	Decreasing capture rate, decreasing to a positive value.
(c)	$\beta_k = \frac{\omega k+1}{\phi k^2+\psi k}$	Decreasing capture rate, decreasing to zero.

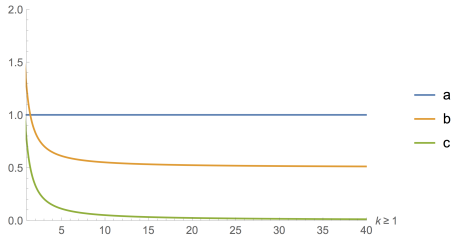

Figure 3.4: The capture rate types plotted with parameter values $\psi = 1, \phi = 0.7, \omega = 0.3$.

Rate (a) is a case of a capture rate independent of the cluster size. This could mean that the predator is well adapted and is able to adjust it's tactics in different sized clusters or that the prey individuals are ineffectual at preventing the capture even if they show up. Rates (b) and (c) are both decreasing as the cluster size increases, i.e. the defense is working. The difference is that in rate (b), the predator still has a chance of capture even in bigger clusters, but in (c) the defense is so effective in big clusters that the the chance of capture decreases to zero.

If the capture rate is constant, the functional response is of Holling type II as seen in the first picture in figure 3.5 on the next page. If the capture rate is decreasing with increasing cluster size k, the functional response will be a non-monotonous functional response. The middle picture in figure 3.5 shows the response with capture rate (b) and the last picture with (c).

In figure 3.6 we see that in the limit the functional response with a capture rate that decreases to a constant, (b), saturates at a positive value in the limit and with a capture rate that decreases to zero, (c), the functional response also decreases to zero.

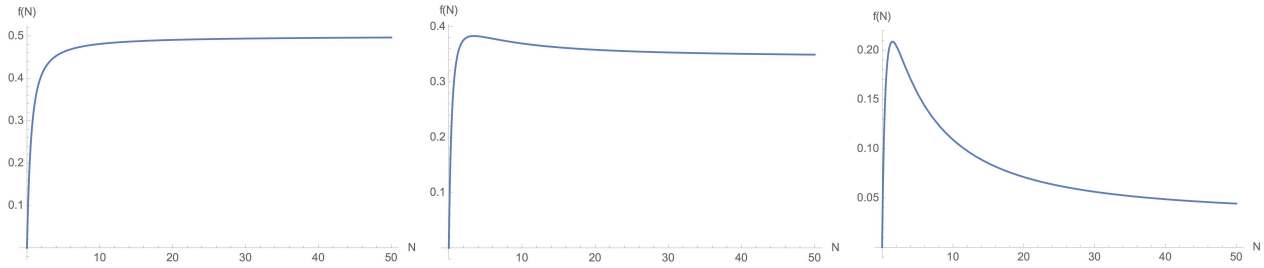

Figure 3.5: Left: constant capture rate (a), middle: capture rate decreasing to a positive value (b), right: capture rate decreasing to zero (c). All plotted with parameter values: $\frac{\alpha}{N} = 2$, $\gamma = 1.5$,, $h = 1$.

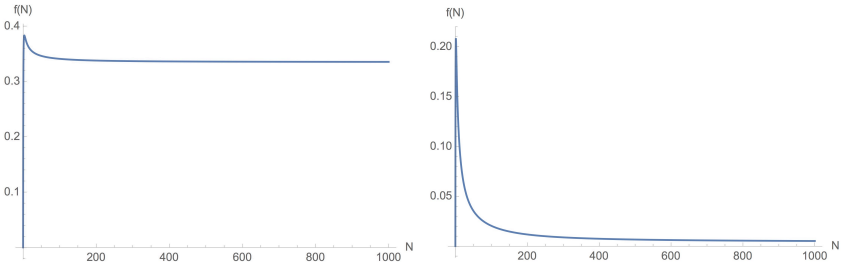

Figure 3.6: Left: capture rate decreasing to a positive value, right: capture rate decreasing to zero.

The condition for the functional response to have a local maximum, i.e. being non-monotonous is that the capture rate is decreasing. The derivative of the functional response with respect to prey density N will always be zero in the limit, but if β_k decreases it will also have a zero value at a local maximum. On the left in figure 3.7 the derivative of the functional response is plotted with a constant capture rate and in the middle figure it's plotted with a decreasing capture rate. The rightmost figure is also plotted with a decreasing capture rate, and it shows how the derivative becomes zero in the limit also here but first taking negative values.

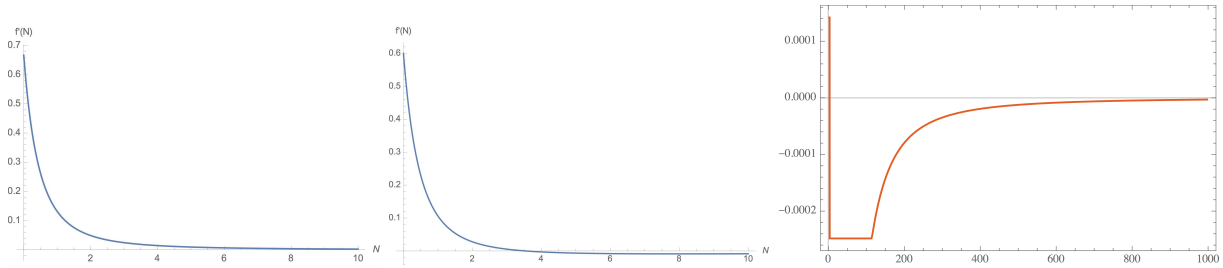

Figure 3.7: The derivative of the functional response with respect to prey density N. Left: constant capture rate, middle and right: decreasing capture rate.

The saturating value in the case of the constant capture rate is $\frac{\beta}{1+h\beta}$. To find the conditions for the different saturating values of the non-monotonous functional response we look at the expression for $f(N)$.

$$
\begin{aligned}
f(N) &= \frac{\sum_{k=1}^{\infty} \beta_k \, \lambda_-(N)^k}{\sum_{k=0}^{\infty} \lambda_-(N)^k + h \sum_{k=1}^{\infty} \beta_k \, \lambda_-(N)^k} = \frac{\sum_{k=1}^{\infty} \beta_k \, \lambda_-(N)^k}{\frac{1}{1-\lambda_-(N)} + h \sum_{k=1}^{\infty} \beta_k \, \lambda_-(N)^k} \\
&= \frac{1}{\frac{1}{(1-\lambda_-(N)) \sum_{k=1}^{\infty} \beta_k \, \lambda_-(N)^k} + h} \qquad (3.9)
\end{aligned}
$$

There are three valid options for the limit of $f(N)$. It can be finite and strictly positive, zero or infinite. However, for the denominator of (3.9) to be zero, the fraction $\frac{1}{(1-\lambda_-(N)) \sum_{k=1}^{\infty} \beta_k \, \lambda_-(N)^k}$ would have to be equal to $-h$, and we know it only takes positive values. So, the functional response can not explode to infinity.

We know that $\lim_{N\to\infty} (1 - \lambda_-(N)) = 0$, so the limit of the fraction in the denominator of (3.9) depends on the power series $\sum_{k=1}^{\infty} \beta_k \, \lambda_-(N)^k$.

If the radius of convergence for the the power series is more than one, it means that the power series converges for every possible value of $\lambda_-(N)$ for sufficiently large K, since $\lambda_-(N)$ is always less than one.

$$
\begin{aligned}
& \lim_{N\to\infty} (1 - \lambda_-(N)) \sum_{k=1}^{\infty} \beta_k \, \lambda_-(N)^k = 0 \\
\Leftrightarrow \quad & \lim_{N\to\infty} \frac{1}{(1-\lambda_-(N)) \sum_{k=1}^{\infty} \beta_k \, \lambda_-(N)^k} = \infty
\end{aligned}
$$

$$\Leftrightarrow \quad \lim_{N\to\infty} f(N) = 0$$

If the radius of convergence for the the power series is less than one, it means that the power series diverges for some values of $\lambda_-(N)$, as $\lambda_-(N)$ is one in the limit.

$$\begin{aligned} & 0 < \lim_{N\to\infty} (1-\lambda_-(N)) \sum_{k=1}^{\infty} \beta_k \, \lambda_-(N)^k \leq \infty \\ \Leftrightarrow \quad & 0 \leq \lim_{N\to\infty} \frac{1}{(1-\lambda_-(N)) \sum_{k=1}^{\infty} \beta_k \, \lambda_-(N)^k} < \infty \\ \Leftrightarrow \quad & 0 < \lim_{N\to\infty} f(N) < \infty \end{aligned}$$

So, if $\limsup_{k\to\infty} |\beta_k|^{\frac{1}{k}} < 1$, the power series has a radius of convergence of more than one and the functional response is zero in the limit. Otherwise, the functional response saturates at a positive but finite value.

3.2.2 Stability of the quasi-equilibrium

For a linear system we look at the eigenvalues of the Jacobi matrix to study the stability of it's equilibrium. If all the eigenvalues have negative real parts, the equilibrium is stable. If even one of the eigenvalues have a positive real part the equilibrium is unstable. If there are eigenvalues with zero real part, the equilibrium is non-hyperbolic and one has to look more carefully at happens around the equilibrium.

Maximum cluster size finite, $K < \infty$

For the case where there is a maximum cluster size, K, the Jacobi matrix is of dimension $(K+1) \times (K+1)$.

$$J(\hat{P}_k) = \begin{pmatrix} -aN & b+c & c & c & \cdots & c \\ aN & -aN-b-c & b & 0 & & 0 \\ 0 & aN & -aN-b-c & b & & 0 \\ \vdots & & & & \ddots & \vdots \\ 0 & 0 & & aN & -aN-b-c & b \\ 0 & 0 & \cdots & 0 & aN & -b-c \end{pmatrix}$$

We see that the Jacobi matrix is off-diagonally non-negative, so we make the following transformation to make it fully non-negative. Here, μ is a constant real number, and I is the identity matrix of same dimensions as $J(\hat{P}_k)$.

$$A = J(\hat{P}_k) + \mu I \qquad \Leftrightarrow$$

$$A = \begin{pmatrix} -aN+\mu & b+c & c & c & \cdots & c \\ aN & -aN-b-c+\mu & b & 0 & & 0 \\ 0 & a & -aN-b-c+\mu & b & & 0 \\ \vdots & & & & \ddots & \vdots \\ 0 & 0 & & aN & -aN-b-c+\mu & b \\ 0 & 0 & \cdots & 0 & aN & -b-c+\mu \end{pmatrix}$$

Theorem 3.10. (The Perron-Frobenius theorem) *Let A be an irreducible matrix, where all it's elements a_{ij} are non-negative. Then the following statements hold.*

1. *A has a positive, real eigenvalue $r(A)$, called the Perron-Frobenius root, such that all other eigenvalues of A satisfy*

$$|\lambda| < r(A) \ .$$

2. *The Perron-Frobenius root is a simple eigenvalue, i.e. $r(A)$ is a simple root of the characteristic polynomial of A.*

3. *There exists an eigenvector v of A with eigenvalue $r(A)$, such that all components of v are positive.*

4. *There are no other non-negative eigenvectors except multiples of v.*

Now A is a non-negative matrix for any $\mu > aN+b+c$, for which the Perron-Frobenius theorem 3.10 holds. The Perron-Frobenius theorem states that a non-negative matrix has a strictly positive, simple, and real maximum eigenvalue called the Perron-Frobenius root, which I will denote by $r(A)$. For the Perron-Frobenius root the following properties hold.

1. $r(A) = r(A^T)$
2. $\min\limits_i \sum\limits_{j=1}^{K+1} a_{ij} \leq r(A) \leq \max\limits_i \sum\limits_{j=1}^{K+1} a_{ij}$ where the a_{ij} are the matrix elements of A

The second property means that the Perron-Frobenius root is sandwhiched between the minimum and maximum of the row sums of the matrix. From the first and second property together it follows that $r(A)$ is also between the column sums of the matrix since the row sums of a matrix are the same as the column sums of it's transpose.

3. $\min_j \sum_{i=1}^{K+1} a_{ij} \leq r(A) \leq \max_j \sum_{i=1}^{K+1} a_{ij}$

We notice that all the column sums of matrix A are exactly μ, so μ must also be the Perron-Frobenius root of A.

$$\mu \leq r(A) \leq \mu \quad \Leftrightarrow \quad r(A) = \mu$$

For our original matrix, $J(\hat{P}_k)$, the following relation holds for all it's eigenvalues λ and the eigenvalues of the transformation A.

$$\lambda = \nu - \mu \ , \quad \text{where } \nu \text{ is an eigenvalue of } A \tag{3.11}$$

Especially, for the maximum eigenvalue of $J(\hat{P}_k)$ the following is true.

$$\lambda_{max} = \nu_{max} - \mu = r(A) - \mu = 0$$

We now know that λ_{max} is a unique, real and zero eigenvalue, because there are no eigenvalues of $J(\hat{P}_k)$ for which (3.11) does not hold. Also, all other eigenvalues must have a real part that is less than zero. In fact, λ_{max} has all the same properties that a Perron-Frobenius root has.

To know what the dynamics are on the long time-scale, we have to look at the dynamics on the slow manifold corresponding to the zero eigenvalue. We know that the slow manifold is attracting, because all the other eigenvalues have a negative real part. The slow manifold is spanned by the eigenvector corresponding to the zero eigenvalue.

$$J(\hat{P}_k)\underline{x} = 0 \ , \quad \text{where } \underline{x} \text{ is a vector in } \mathbb{R}^{K+1} \tag{3.12}$$

The eigenvector we are looking for is the non-zero solution of (3.12). But because the cluster dynamic is a system of linear differential equations, equation (3.12) also defines it's set of equilibrium equations. We've established earlier that $\hat{P}_k$ is the unique non-zero solution of the equilibrium equations, which means that the equilibrium distribution is equilvalent to the slow manifold. Also, the solution of the system which stays on the slow manifold is (3.13), and it is clearly stationary in time.

$$P_k(t) = \underline{x}e^{0*t} = \hat{P}_k \qquad \text{for all } 0 \leq k \leq K \tag{3.13}$$

In conclusion, because all other eigenvalues of the Jacobi matrix have a negative real part, the dynamics of the system will converge to the slow manifold corresponding to the simple and real zero eigenvalue. The slow manifold is the equilibrium distribution $\hat{P}_k$, so the equilibrium is stable. Moreover, it is stable for an arbitrarily big, but finite maximum cluster size.

Next step is to try to prove the same for the equilibrium in an untruncated version of the cluster dynamics.

Maximum cluster size infinite, $K = \infty$

The following is a suggestion for a way of completing the proof, however I was not able to prove stability. I leave this here as a sort of footnote.

The Jacobi matrix of the system takes the following form in a system with no maximum cluster size.

$$J(\hat{P}_k) = \begin{pmatrix} -aN & b+c & c & c & c & \\ aN & -aN-b-c & b & 0 & 0 & \\ 0 & aN & -aN-b-c & b & 0 & \cdots \\ 0 & 0 & aN & -aN-b-c & b & \\ 0 & 0 & 0 & aN & -aN-b-c & \\ & & \vdots & & & \ddots \end{pmatrix}$$

Like in the previous section, the Jacobi matrix is an off-diagonally non-negative matrix. However it is now an "infinite-dimensional" square matrix, and straight forward linear algebra does not apply. By the same simple transformation we can still make it a fully non-negative matrix by adding a constant μ ($\mu > aN + b + c$) to the diagonal. I call the transormed matrix A_∞.

$$A_\infty = J(\hat{P}_k) + \mu I \quad \Leftrightarrow$$

$$A_\infty = \begin{pmatrix} -aN+\mu & b+c & c & c & \\ aN & -aN-b-c+\mu & b & 0 & \\ 0 & aN & -aN-b-c+\mu & b & \cdots \\ 0 & 0 & aN & -aN-b-c+\mu & \\ & & \vdots & & \ddots \end{pmatrix}$$

Theorem 3.14. (The Krein-Rutman theorem) *Let X be a Banach space, and let $K \subset X$ be a convex cone such that K-K is dense in X. Let $T : X \to X$ be a non-zero positive compact operator and assume that it's spectral radius r(T) is strictly positive. Then r(T) is an eigenvalue of T with positive eigenvector.*

The generalisation of the Perron-Frobenius theorem to the infinite dimensional case is the Krein-Rutman theorem 3.14, which applies to compact operators [11]. I made an attempt at applying Krein-Rutman theorem to the linear operator (3.15) defined by the matrix A_∞.

$$F(x) = A_\infty(x) \qquad F : X \to X \tag{3.15}$$

In (3.15) X is the infinite dimensional space $\mathbb{R}^\infty$, equipped with an operator norm. Then, the space X is a Banach space.

We know that the matrix A_∞ is the limit of compact operators F_m, defined by the matrices A_m, when $m \to \infty$. The A_m are matrices with a $m \times m$ dimensional truncated version of A_∞ in the upper left corner, zero otherwise. So, we know the operator F is compact as well.

$$F_m(X) = A_m x \qquad F_m : X \to X \tag{3.16}$$

$$A_m = \begin{pmatrix} -aN+\mu & b+c & c & 0 & \\ aN & -aN-b-c+\mu & b & 0 & \\ 0 & aN & -aN-b-c+\mu & 0 & \cdots \\ 0 & 0 & 0 & 0 & \\ & & \vdots & & \ddots \end{pmatrix}$$

Also, $\mathbb{R}^\infty_+$, where $0 \in \mathbb{R}_+$ defines a convex cone, which the linear operator F maps non-emptively into itself.

So it seems Krein-Rutman theorem might be a feasible way of generalising the method from the finite case. Unfortunately there is a long way to go from here to the full proof.

Conclusions

In the case of positive, constant rates a (coagulation), b (fragmentation) and c (cluster bursting), the functional response was found to take a dome-shaped form, decreasing to zero under certain circumstances, or the form of Holling type II functional response. The determining factor for which type of functional response the model gives rise to is whether the predator's attack rate is dependent on the cluster size or not.

The cluster dynamics truncated with a maximum size for the clusters was found to have a unique and stable equilibrium for arbitrarily large maximum cluster sizes. The stability analysis for cluster dynamics with no maximum cluster size was not successful, even though there is reason to believe the results for the truncated system is generalizable to that case.

3.3 Special case: two cluster dynamic rates

In this section, I will look at a special case of the cluster dynamics where prey individuals only join clusters but don't leave until the whole cluster breaks up, i.e. $b = 0$, $a > 0$, $c > 0$. In this case the prey are more stubborn and loyal and won't leave another prey in trouble. Here the rates can be dependent on the cluster size k. The dynamical system on the cluster dynamics time scale is a little simpler now.

$$\begin{cases} \dot{P}_0 = -a_0 N P_0 + \sum_{k=1}^{K} c_k P_k \\ \dot{P}_k = a_{k-1} N P_{k-1} - (a_k N + c_k) P_k \qquad \text{for } 0 < k < K \\ \dot{P}_K = a_{K-1} N P_{K-1} - c_K P_K \end{cases} \tag{3.17}$$

In this case solving the quasi-equilibrium is a straight-forward task compared to the previous case and yields the following. Stability of this is proven in section 3.3.2, again only for the case of finite cluster size. The equilibrium is unique because of the linearity of the system.

$$\hat{P}_k = \left(\prod_{q=0}^{k-1} \frac{a_q N}{a_{q+1} N + c_{q+1}} \right) \hat{P}_0$$

The equilibrium cluster size distribution depends on the rates a_k and c_k. I will again look at what forms the rates can realistically take, but without deriving them from individual level processes.

The predator attack rate a_0 must always be positive. For the prey joining rates a_k ($k \geq 1$), I will consider four different options, shown on the left in figure 3.8, and for the cluster break up rate c_k I consider three different options, shown in the same figure on the right.

(d) $a_k = \psi$ Constant prey joining rate.

(e) $a_k = \frac{\phi k^2 + \psi k}{\omega k + 1}$ Increasing prey joining rate.

(f) $a_k = \frac{\psi k}{\omega k + 1}$ Increasing and saturating joining rate.

(g) $a_k = \begin{cases} 4 \sin\left(\frac{k}{10}\right) & 0 < k \leq 10\pi \\ 0 & k > 10\pi \end{cases}$ Dome-shaped prey joining rate.

(h) $c_k = \psi$ Constant cluster break up rate.

(i) $c_k = \frac{\phi k^2 + \psi k}{\omega k + 1}$ Increasing cluster break up rate.

(j) $c_k = \frac{\psi k}{\omega k + 1}$ Increasing and saturating cluster break up rate.

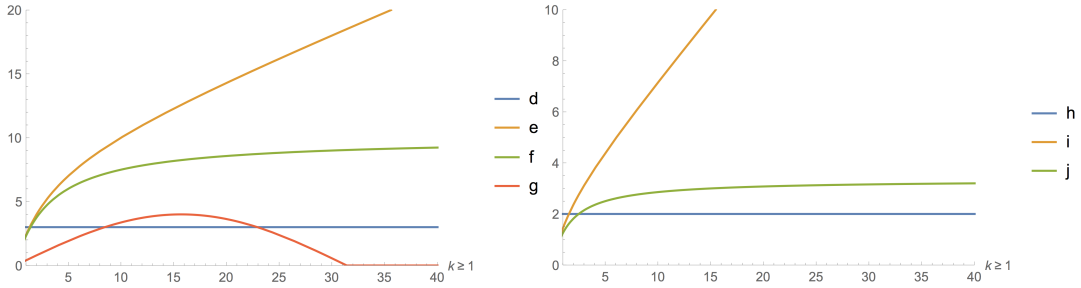

Figure 3.8: Left: Prey joining rate a_k types plotted with parameter values $\psi = 3$, $\phi = 0.1$, $\omega = 0.3$. Right: cluster break up rate c_k types plotted with parameter values $\psi = 2$, $\phi = 0.3$, $\omega = 0.6$.

A possible interpretation of the prey joining rates (f) and (g) in the list above is that the prey can count up to a certain amount of individuals in the cluster and take that into account when deciding whether to join or not. If the rate is equal to (e), the prey gets more encouraged to help out the more individuals there are in the cluster already. In the case of the constant attack rate the decision making of the prey is independent of what the others are doing.

Below in figure 3.9 the equilibrium cluster size distribution is shown for rates increasing with k and constant rates.

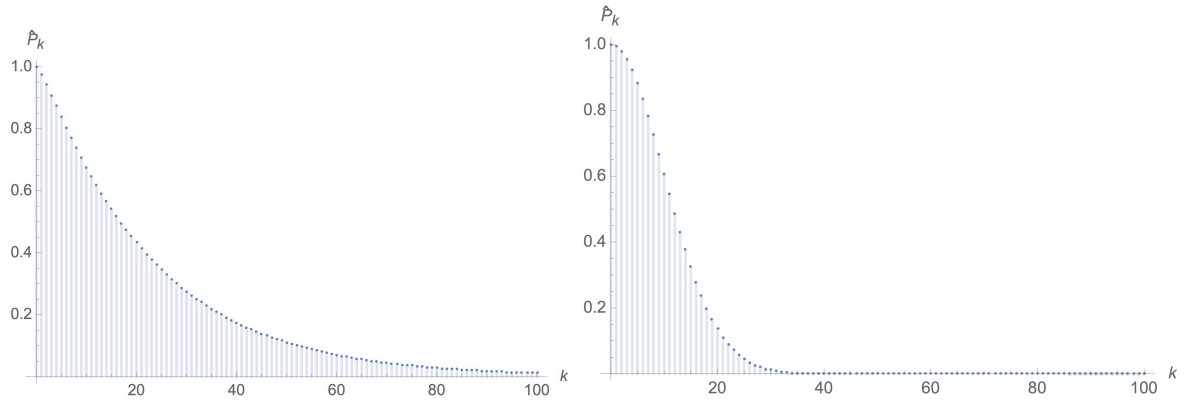

Figure 3.9: Left: equilibrium distribution with prey joining rate (f) and cluster break up rate (j), same parameter values used as in figure 3.8. Right: equilibrium distribution with constant rates $a_k = 0.6$ and $c_k = 0.3$. ($a_0 = 3,\ N = 100,\ P_0 = 1,\ K = 100$ used for both.)

As before, inserting the expression for the quasi-equilibrium into (3.3) on page 19 gives a functional response dependent only on the prey density.

$$f(N) = \frac{\sum_{k=1}^{K} \beta_k \hat{P}_k}{\sum_{k=0}^{K} \hat{P}_k + h \sum_{k=1}^{K} \beta_k \hat{P}_k} = \frac{\sum_{k=1}^{K} \beta_k \left(\prod_{q=0}^{k-1} \frac{a_q N}{a_{q+1} N + c_{q+1}} \right)}{\sum_{k=0}^{K} \left(\prod_{q=0}^{k-1} \frac{a_q N}{a_{q+1} N + c_{q+1}} \right) + h \sum_{k=1}^{K} \beta_k \left(\prod_{q=0}^{k-1} \frac{a_q N}{a_{q+1} N + c_{q+1}} \right)} \tag{3.18}$$

3.3.1 The shape of the functional response

The shape of the functional response in this case depends on what the three parameters β_k, a_k and c_k are chosen to be. I use the same options for the capture rate β_k as in section 3.2.1, and the options from figure 3.8 for prey joining rate a_k and cluster break up rate c_k (parameter values the same as in figure 3.8).

This gives 36 different parameter combinations, but it turns out that also in this case the deciding factor for the shape of the functional response is the predator capture rate.

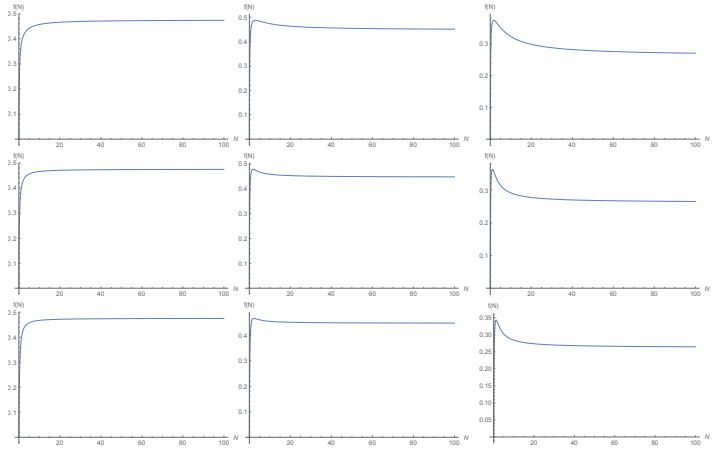

Figure 3.10: The functional response $f(N)$ plotted as a function of prey density N for all parameter combinations for increasing prey joining rate ((e) on p. 32).
Capture rate β_k: left column constant, middle column decreasing, right column decresing to zero (cases (a), (b) and (c) on p. 23).
Cluster break up rate ck: 1. row increasing, 2. row increasing and saturating, 3. row constant (cases (i), (j) and (h) on p. 32).
For all cases here $h = 1$, $a_0 = 3$ and maximum cluster size $K = 32$.

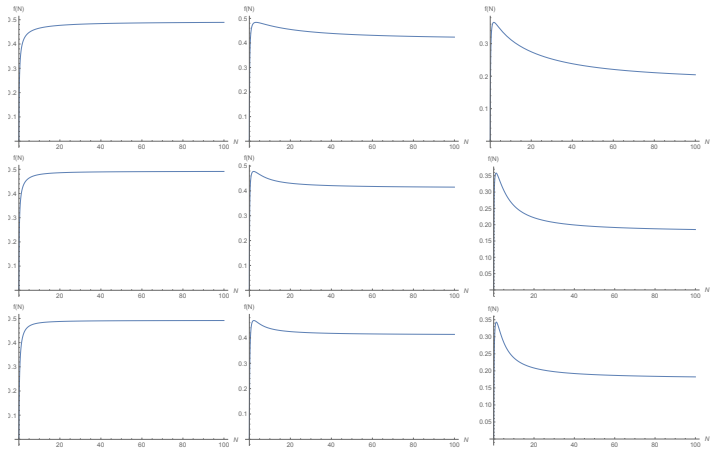

Figure 3.11: The functional response $f(N)$ plotted as a function of prey density N for all parameter combinations for dome-shaped prey joining rate, case (g) on p. 32.
Capture rates β_k and cluster break up rates ck arranged in columns and rows same way as in figure 3.10. Same values for parameters h, a_0 and K also.

In figure 3.10 the resulting functional responses are shown for all nine parameter

combinations for strictly increasing prey joining rate ((*e*) in figure 3.8). In figure 3.11 the combinations for the dome-shaped prey joining rate (*f*) are shown. The combinations for the two other prey joining rates considered, (*d*) and (*g*), give similar results. For those combinations the functional response only differs from the results in figures 3.10 and 3.11 in the saturation value and slope. However, no combination of parameters yields a functional response decreasing to zero.

As in the previous special case, the constant capture rate gives a Holling type II functional response independent of the other rates. The decreasing capture rate gives a non-monotonous functional response in both special cases, but in this latter one the saturating value for the functional response stays positive for all capture rates. Also in this case there will only be a local maximum, i.e. a zero value of the derivative of $f(N)$ that is not at the asymptote, if the capture rate β_k is decreasing as k increases.

Again, we're going to look at the expression for the functional response to see what happens in the limit $N \to \infty$. The functional response can be written into the following form where we can see how the value in the limit depends on the relationship between the two series.

(3.19)
$$f(N) = \frac{\sum_{k=1}^{K} \beta_k \left(\prod_{q=0}^{k-1} \frac{a_q N}{a_{q+1} N + c_{q+1}} \right)}{\sum_{k=0}^{K} \left(\prod_{q=0}^{k-1} \frac{a_q N}{a_{q+1} N + c_{q+1}} \right) + h \sum_{k=1}^{K} \beta_k \left(\prod_{q=0}^{k-1} \frac{a_q N}{a_{q+1} N + c_{q+1}} \right)} = \frac{1}{\frac{\sum_{k=0}^{K} \left(\prod_{q=0}^{k-1} \frac{a_q N}{a_{q+1} N + c_{q+1}} \right)}{\sum_{k=1}^{K} \beta_k \left(\prod_{q=0}^{k-1} \frac{a_q N}{a_{q+1} N + c_{q+1}} \right)}} + h$$

We see that the limit of $f(N)$ equals zero if the limit of the expression (3.20) is infinite, finite if the limit of (3.20) is finite, and infinite if the limit of (3.20) is $-h$. The latter is clearly not possible and if the limit is finite it's also positive.

(3.20)
$$\frac{\sum_{k=0}^{K} \left(\prod_{q=0}^{k-1} \frac{a_q N}{a_{q+1} N + c_{q+1}} \right)}{\sum_{k=1}^{K} \beta_k \left(\prod_{q=0}^{k-1} \frac{a_q N}{a_{q+1} N + c_{q+1}} \right)}$$

For all realistic prey joining rates a_k, except the dome-shaped rate, the following holds.

$$a_q N \leq a_{q+1} N < a_{q+1} N + c_{q+1} \qquad \text{for all } q \geq 1,\ N \geq 0$$

$\Leftrightarrow$

$$\frac{a_q N}{a_{q+1} N + c_{q+1}} < 1 \qquad \text{for all } q \geq 1,\ N \geq 0$$

$\Leftrightarrow$

$$\lim_{N\to\infty} \frac{a_q N}{a_{q+1}N + c_{q+1}} < 1 \quad \Leftrightarrow \quad \lim_{N\to\infty} \sum_{k=0}^{K} \left(\prod_{q=0}^{k-1} \frac{a_q N}{a_{q+1}N + c_{q+1}} \right) < \infty \tag{3.21}$$

The dome-shaped joining rate a_k goes to zero, so the right hand side of (3.21) clearly holds in that case as well.

We see that the denominator of (3.20) is always positive and more than zero, so a necessary condition for the expression to have an infinite limit is if the numerator is infinity in the limit. But we have just observed that the numerator has a finite limit for all rates a_k considered realistic, so the functional response can only have a finite, strictly positive limit as prey density grows.

3.3.2 Stability of the quasi-equilibrium

For the case when there is a maximum cluster size and when there's not, the stability analysis of the equilibrium is completely analogous to section 3.2.2.

Maximum cluster size finite, $K < \infty$

$$J_K(\hat{P}_k) = \begin{pmatrix} -a_0N & c_1 & c_2 & c_3 & c_4 & \cdots & c_K \\ a_0N & -a_1N - c_1 & 0 & 0 & 0 & & 0 \\ 0 & a_1N & -a_2N - c_2 & 0 & 0 & & 0 \\ 0 & 0 & a_2N & -a_3N - c_3 & 0 & & \vdots \\ 0 & 0 & 0 & a_3N & -a_4N - c_4 & & 0 \\ \vdots & & & & & \ddots & 0 \\ 0 & 0 & 0 & \cdots & 0 & a_{K-1}N & -c_K \end{pmatrix}$$

We make the transformation of the Jacobi matrix to a non-negative matrix again.

$$A = J(\hat{P}_k) + \mu I$$

In the exact same way as in section 3.2.2, the columns sums of the matrix A are equal to μ, so the Perron-Frobenius root is also equal to μ.

$$r(A) = \mu$$

Following from that, the maximum eigenvalue of the Jacobi matrix, λ_{max}, is zero, and it is simple and real.

$$\lambda_{max} = r(A) - \mu = 0$$

Again, the non-zero eigenvector $\underline{x}$ corresponding to the zero eigenvalue spans the slow manifold, and is equal to the equilibrium solution.

$$J(\hat{P}_k)\underline{x} = 0 \quad \Leftrightarrow \quad \underline{x} = \hat{P}_k$$

Also here the unique equilibrium solution of the linear system is stable because it itself is an attracting slow manifold.

Maximum cluster size infinite, $K = \infty$

Stability for this case left an open question.

Conclusions

In the case of non-constant rates a_k (coagulation, c_k (cluster bursting) and with $b_k = 0$ (fragmentation), the functional response was found to take a dome-shaped form, however never decreasing to zero, or the form of Holling type II functional response. The determining factor for which type of functional response the model gives rise to is also in this case whether the predator's attack rate β_k is dependent on the cluster size or not.

Results of the stability analysis are qualitatively the same as in previous special case (section 3.2. The truncated cluster dynamics with a maximum size for the clusters was found to have a unique and stable equilibrium for arbitrarily large maximum cluster sizes. The stability analysis for the cluster dynamics with no maximum cluster size was not successful, even though there is reason to believe the results for the truncated system is generalizable to that case.

Chapter 4

Discussion

In this thesis the functional response was derived from the individual level processes in a prey-predator system with active defense from the prey. The model was assumed to have three characteristic time-scales, which held up in further analysis. The dynamics on the successive timescales (from fast to slow) were called the cluster formation dynamics, the searching-handling cycle of the predator dynamics and the population level dynamics.

The prey defense was modelled as a generelized Becker-Döring process, and in the case of a finite maxium cluster size it was found to have a stable equilibrium. The stability in the case of no truncation of the cluster sizes turned ut to be a more complicated matter, and in the end was left as an open question.

It would be interesting, although out of the scope of this thesis to look at e.g., the resulting actual population dynamics, a modelling approach to the cluster formation parameters and evolution of cooperative traits of the prey.

4.1 Other types of cooperation

The cooperation of prey seen in this model is only one special type of cooperative defense of the prey. Another version of active group defense is modelled in an article by Jeschke and Tollrian [10], where the predator gets confused by swarms of prey and makes it less succesfull in it's attacks. They found that predator confusion did not necessarily lead to a dome-shaped functional response.

The same was found in this thesis, although the case where the functional response becomes monotonous is the one where cluster size does not affect the predator's capture rate, which not too realistic. The predator confusion of the article and the active prey defense here are qualitatively not too different, so this model can be seen as a mechanical derivation of the results validated with data in the article.

On the other hand, predators can also cooperate. In an article by Alves and Hilcker [1], the predator hunting cooperation was shown to promote Allee effects, i.e. that that there is a critical population density under which the population can not presist. In this thesis the predators were modelled as predators hunting alone, but it could be extended to cooperating predators as well to counteract the cooperation of the prey.

4.2 An unrealistic example

For the capture rate of the predator we only considered a constant β_k or decreasing capture rate β_k as $k \to \infty$. In theory, one could imagine a predator to have an "optimal cluster size" for capture. An exaggerated example of this is shown on the left in figure 4.1, where the capture rate reaches it's maximum at cluster size 30. The capture rate was considered to become zero in the limit.

The expression for the functional response used here is the same as in section 3.2. This capture rate results in a functional response with similar shape to the Holling type III functional response initially, and a hump-shaped functional resopnse in the limit.

I include this here as an example that a wide variety of shapes for the functional response can be engineered with such a great degree of freedom for the different parameters as in this model, so the parameters should be chosen carefully.

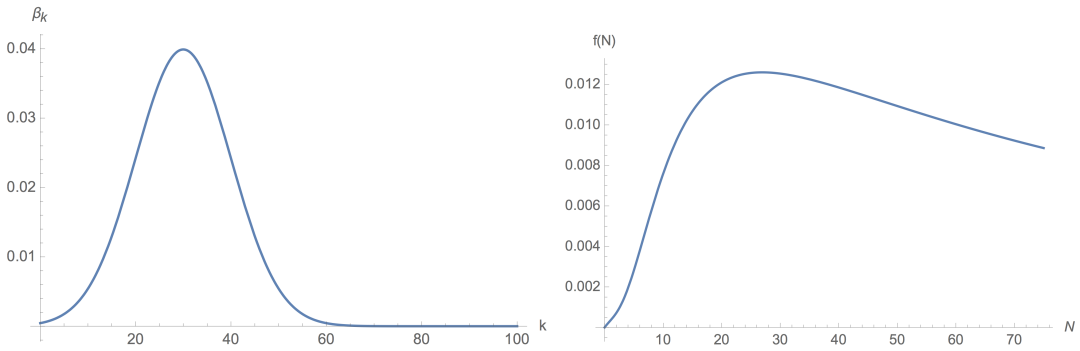

Figure 4.1: $\frac{\alpha}{N} = 2, \gamma = 2, h = 1$ Left: the attack rate as the normal distribution N(30,10) Right: The type V functional response

Bibliography

[1] Mickaël Teixeira Alves and Frank M Hilker. Hunting cooperation and allee effects in predators. *Journal of Theoretical Biology*, 419:13–22, 2017.

[2] R. Becker and W. Döring. Kinetische behandlung der keimbildung in übersättigten dämpfen. *Annalen der Physik*, 416(8):719–752, 1935.

[3] J. R. Beddington. Mutual interference between parasites or predators and its effect on searching efficiency. *Journal of Animal Ecology*, 44(1):331–340, 1975.

[4] D. L. DeAngelis, R. A. Goldstein, and R. V. O'Neill. A model for tropic interaction. *Ecology*, 56(4):881–892, 1975.

[5] GF Gause, NP Smaragdova, and AA Witt. Further studies of interaction between predators and prey. *The Journal of Animal Ecology*, pages 1–18, 1936.

[6] S. A. H. Geritz and M. Gyllenberg. Group defence and the predator's functional response. *Journal of Mathematical Biology*, 66(4):705–717, 2013.

[7] David M Grobman. Homeomorphism of systems of differential equations. *Doklady Akademii Nauk SSSR*, 128(5):880–881, 1959.

[8] Philip Hartman. A lemma in the theory of structural stability of differential equations. *Proceedings of the American Mathematical Society*, 11(4):610–620, 1960.

[9] C. S. Holling. Some characteristics of simple types of predation and parasitism. *The Canadian Entomologist*, 91(7):385–398, 1959.

[10] Jonathan M. Jeschke and Ralph Tollrian. Effects of predator confusion on functional responses. *Oikos*, 111(3):547 – 555, 2005.

[11] Mark Grigor'evich Krein and Mark A Rutman. Linear operators leaving invariant a cone in a banach space. *Uspekhi Matematicheskikh Nauk*, 3(1):3–95, 1948.

[12] Alfred J Lotka. The growth of mixed populations: two species competing for a common food supply. *Journal of the Washington Academy of Sciences*, 22(16/17):461–469, 1932.

[13] A. M. Lyapunov. The general problem of motion stability. *Annals of Mathematics Studies*, 17, 1892.

[14] R. H. MacArthur M. L. Rosenzweig. Graphical representation and stability conditions of predator-prey interactions. *The American Naturalist*, 97(895):209–223, 1963.

[15] Leonor Michaelis and Maud L Menten. Die kinetik der invertinwirkung. *Biochem. z*, 49(333-369):352, 1913.

[16] Leslie A. Real. The kinetics of functional response. *The American Naturalist*, 111(978):289–300, 1977.

[17] Vito Volterra. Variations and fluctuations of the number of individuals in animal species living together. *ICES Journal of Marine Science*, 3(1):3–51, 1928.